

Nickel-Catalyzed Cycloisomerization of 1,5-Allenynes

Juan C. Nieto-Carmona,^a Inés Manjón-Mata,^a M. Teresa Quirós,^{b,*}
Gema Caballero-Santiago,^a Fernando Pérez-Maseda,^a and Diego J. Cárdenas^{a,*}

^a Department of Organic Chemistry, Facultad de Ciencias, Universidad Autónoma de Madrid, Institute for Advanced Research in Chemical Sciences (IAdChem), Red ORFEO-CINQA. Av. Francisco Tomás y Valiente 7, Campus de Cantoblanco, 28049, Madrid, Spain

E-mail: diego.cardenas@uam.es

^b Department of Organic Chemistry and Inorganic Chemistry, Facultad de Farmacia, Universidad de Alcalá, Campus Universitario. Ctra. Madrid-Barcelona, Km. 33,600. Alcalá de Henares, 28871, Madrid, Spain

E-mail: teresa.quirós@uah.es

Manuscript received: September 26, 2023; Revised manuscript received: November 15, 2023;

Version of record online: ■■■, ■■■



Supporting information for this article is available on the WWW under <https://doi.org/10.1002/adsc.202301090>

© 2023 The Authors. Advanced Synthesis & Catalysis published by Wiley-VCH GmbH. This is an open access article under the terms of the Creative Commons Attribution Non-Commercial NoDerivs License, which permits use and distribution in any medium, provided the original work is properly cited, the use is non-commercial and no modifications or adaptations are made.

Abstract: We report the Ni-catalyzed cycloisomerization of 1,5-allenynes. Substrates containing terminal alkynes afford cyclopentene derivatives, whereas internal alkynes lead to the formation of two consecutive C–C bonds to give fused 5–5 bicyclic compounds. The reaction shows a wide scope. Experimental and computational mechanistic studies suggest a Ni(0)–Ni(II) catalytic cycle. The reaction starts with an oxidative cyclometallation followed by a β -hydrogen elimination. The trans arrangement of alkenyl and hydride ligands is key to allow formation of the second carbocycle.

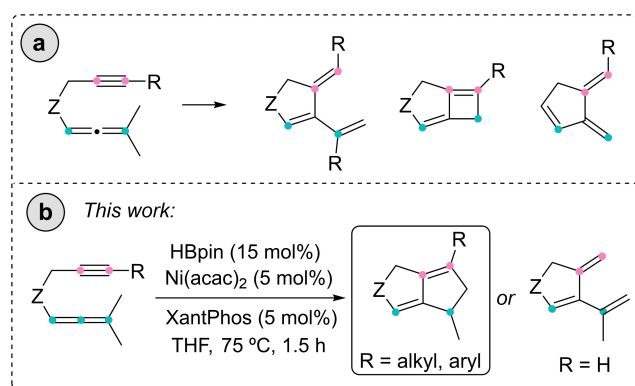
Keywords: Allenes; Nickel; Reaction mechanisms; Cyclization

Introduction

Cycloisomerization reactions are powerful synthetic tools since they provide an increase in the molecular complexity with no generation of by-products. Metal catalysis allows the use of mild conditions and the development of selective transformations. In this context, allenynes have an important role since the reactivity of cumulated dienes allows obtaining of new interesting cycloisomerization products. The use of these compounds, especially 1,6- and 1,7-allenynes, has been widely studied, and different scaffolds are accessible.^[1,2] This is due to the variety of different reaction pathways and activation mechanisms which rely on the reactivity properties of the metal complexes. On the other hand, cycloisomerization of 1,5-allenynes has been less exploited. Although thermal cycloisomerization can take place from these derivatives, metal-catalyzed processes permit further control of the reactions. Catalysts based on Au,^[4] Pt,^[5] Pd,^[6] Rh,^[7] and Ru,^[8] have been used for the cycloisomeriza-

tion of 1,5-allenynes, whereas a single example has been reported using Cu.^[9] In general, simple 1,5-allenynes evolve to cyclopentene derivatives, although Pd-catalysis allows the formation of 5–4 fused bicycles (Scheme 1). The presence of amines, alcohols and aromatic rings on the allenyne permits the preparation of more complex structures using Au complexes as catalysts,^[4] taking advantage of the rich reactivity of alkynes in combination with Au.^[10]

Our interest in the development of synthetically useful transformations based on more convenient first-row transition metals,^[11,12] led us to explore the Ni-catalyzed cycloisomerization of 1,5-allenynes. Herein, we report the formation of different cycloisomerization products from 1,5-allenynes. The reaction outcome depends on the presence of a substituent on the distal position of the alkyne. Whereas terminal alkynes provide monocyclic trienes, internal alkynes afford interesting bicyclic derivatives containing 5–5 fused rings, by consecutive formation of two C–C bonds. This kind of scaffold is present in natural products,^[13]



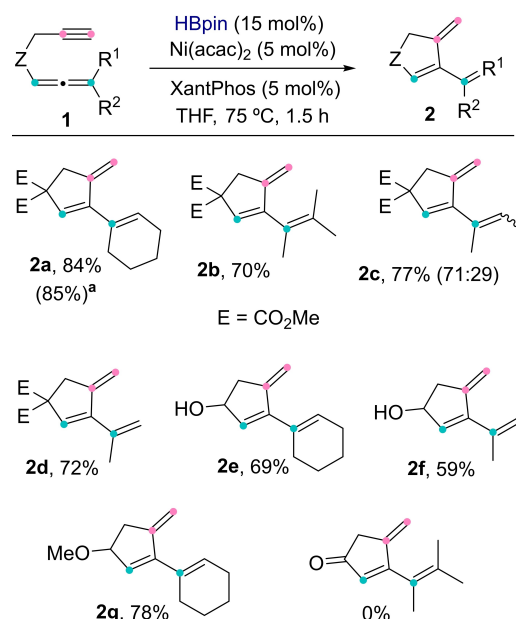
Scheme 1. Possible structures obtained by metal-catalyzed cycloisomerization of 1,5-allenynes.

and biologically active compounds,^[14,15] it has not been reported in the cyclization of other allenynes and can be accessed by this atom-economic transformation employing inexpensive catalyst.

Results and Discussion

During the course of our investigation on Ni-catalyzed borylative cyclization reactions,^[12d] we observed that cycloisomerization derivatives were obtained as by-products. Then, we tried to optimize the conditions for the preparation of such derivatives in the absence of borylating reagent. However, we observed that HBpin was necessary for the cycloisomerization to proceed when using a Ni(II) precatalyst.

We propose that HBpin reduces the starting Ni(II) precatalyst to an active Ni(0) species stabilized by the ligand present (*vide infra*). In our initial experiments, allenyne **1a** was used as the reaction substrate, affording triene **2a** (Scheme 2), which is the kind of derivative observed in the related Cu-catalyzed reactions.^[9] After much experimentation to optimize the reaction conditions (Table 1), **2a** was prepared in 84% yield, using Ni(acac)₂ (5 mol%) and XantPhos (5 mol%) as the catalytic system, and HBpin (15 mol%) as the reducing agent. Initially, we searched for other reducing agents that could activate the precatalyst (not shown in Table 1). Both HBpin and NaBH₄ afforded similar results (72% and 74% yield, respectively), and we considered pinacol borane as a more suitable reagent for practical experimental reasons (solubility and facility to handle and weigh). In contrast, in the presence of LiBH₄, NaHBET₃, and HSi(OMe)₃, the reaction did not take place. We also investigated the effect of the temperature, reaction time and the amount of HBpin (entries 2–9). Higher HBpin amounts allow the reaction to proceed at lower temperature, suggesting a relatively slow Ni(II) reduction (entries 8–9). We realized that just 10 mol% of HBpin was enough for the reaction to proceed without



Scheme 2. Scope of Ni-catalyzed cycloisomerization of 1,5-allenynes with terminal alkyne. [a] Reaction at 1 mmol scale.

Table 1. Optimization of the reaction. Changes in the optimized reaction conditions are shown in entries 2–22.

Ligand	T (°C)	t (h)	HBpin (mol %)	Solvent	Yield (%) ^[a]
1	None				84
2		1	5	DMF	< 40 ^[b]
3	50	1	10	DMF	72
4	50	1	20	DMF	72
5	50	1	50	DMF	73
6	23	20	5	DMF	0
7	23	20	10	DMF	17
8	23	4	50	DMF	58
9	23	1	150	DMF	72
10			10	MeCN	77
11			10	DMF	82
12			15	DMF	84
13			10	THF	82
14			15	MeCN	82
15			10	dioxane	54
16			10	toluene	53
17	^t Bu-XantPhos				7
18	DPE-Phos				23
19	dppf				7
20	bpy				0
21	tpy				0
22	neocuproine				0

^[a] Isolated yields.

^[b] Decomposition products prevented purification.

affecting the yield, which suggests that the sole role of the borane is the reduction of Ni, and that the hydrogen from HBpin does not incorporate into the products. Nevertheless, the purity of HBpin affects the yield, and we decided to keep 15 mol% HBpin for the reproducibility of the reaction. Regarding the effect of the solvent (Table 1, entries 10–16), THF and DMF led to similar yields. MeCN was less effective, and dioxane and toluene afforded poorer results. THF was chosen for the study of the reaction scope for convenience. The use of other bidentate phosphines afforded lower yields, and nitrogen ligands gave no reaction (entries 17–22). We explored the reaction scope by submitting other 1,5-allenynes containing a terminal alkyne, to the optimized reaction conditions.

The process is compatible with the presence of esters (**2a**, **2b**, **2c**, and **2d**), alcohols (**2e** and **2f**) and ether (**2g**) and affords moderate to good yields (Scheme 2). The reaction was not stereoselective when the allene was unsymmetrically substituted (**2c**). The substrate containing a ketone tether did not give the reaction.

Interestingly, when substrate **3a**, containing an internal alkyne, was subjected to the optimized reaction conditions, bicyclic compound **4a** was obtained as the major product (Scheme 3). Distal carbon of the alkyne binds to the initial Me group on the allene to generate the second ring. Formation of triene **2d** was observed although in much lower yield.

We performed additional experiments to try to optimize the yield for this substrate (see Supporting Information). Variations on the Ni precatalyst, ligand and solvent afforded worse results.

We optimized the reaction time so that the conversion was complete (4 h) but not longer, since product decomposition was observed after prolonged heating. To sum up, extending the reaction time was the sole parameter which afforded better results in comparison with the conditions optimized for substrates **2**.

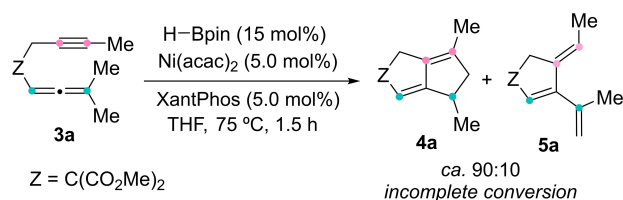
The reaction could be satisfactorily extended to other substrates containing internal alkynes with both alkyl and aryl substitution (Scheme 4). Changes in the substitution of the allene gave a variety of results. Substrate **3a** showed high selectivity towards the formation of the bicyclic derivative **4a** (**4a**:**5a**, 87:13). Selectivity slightly varies when extending the reaction

to 9 h due to products decomposition, and **5a** does not seem to be an intermediate in the formation of **4a**. Allenyne **3b**, which is asymmetrically substituted in the terminal position of the allene with an Et and a Me groups, gave a mixture of 3 isomers (**4b**, **5b** and **5b'**) with high yield. The three products obtained were: the expected bicycle **4b**, the triene coming from the formation of the olefin in the ethyl moiety **5b** (we could not identify if the trisubstituted alkene was *Z* or *E*), and a small amount of the isomer corresponding to the formation of the olefin in the methyl moiety **5b'**. This result suggests that the reaction prefers the mechanism that leads to the more substituted and stable olefin. To corroborate this, the substrate with an ⁱPr and a Me in the terminal position of the allene (**3c**) was subjected to the reaction conditions, and **4c** together with **5c** were obtained in a (68:32) mixture with a high yield. In this case, the tetrasubstituted alkene **5c** was selectively formed, and the formation of the disubstituted olefin (coming from the hydrogen elimination on the methyl group) was not observed. Noteworthy, cyclohexyl derivative **3d** furnished **4d** and **5d** with the inversion of the selectivity (11:89) in a 92% yield. In addition, diene **4d** has two stereogenic centres but only one diastereomer was formed, and a high yield was observed. This implies that the mechanism of the Ni-catalysed cycloisomerization of 1,5-allenynes goes through stereoselective pathways.

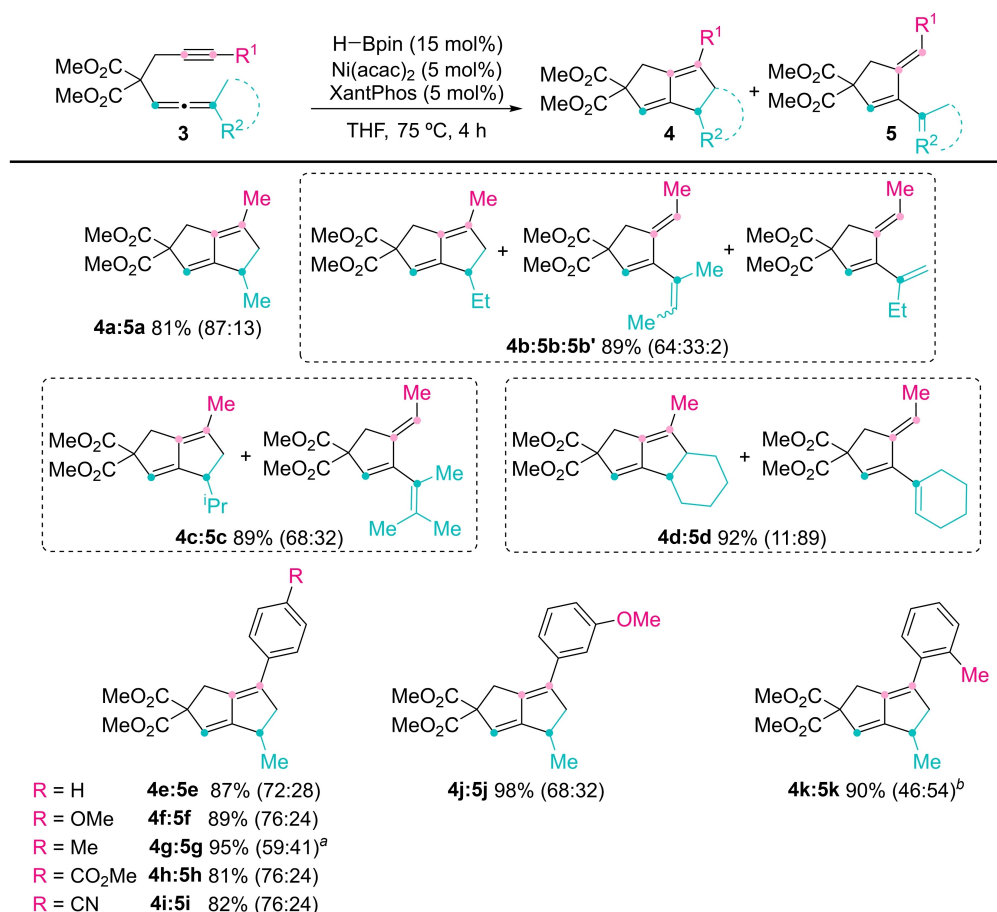
The reaction was broadly applicable for a wide variety of aryl-substituted allenynes, and different functionalities were well tolerated under the optimized conditions. Yields were not affected by the introduction of electron-withdrawing or electron-donating functional groups in the *para* position of the aryl. Products **4e**:**5e**, **4f**:**5f**, **4h**:**5h** and **4i**:**5i** were obtained with high yields and selectivities between 70:30 and 80:20. Neither with *meta*- nor with *ortho*-substituted substrates **3j** and **3k** a detriment of the yield was observed. Products **4j**:**5j** and **4k**:**5k** were isolated with excellent yields. Surprisingly, *para*-methyl and *ortho*-methyl substituted substrates **3g** and **3k** delivered worse selectivities (close to 1:1).

Once the scope of the reaction was explored, we turned our attention to the possible reaction mechanisms. The fact that only 10 mol% of HBpin was necessary for the reaction to proceed, suggests that it was acting just as a hydride source for the activation of the catalyst. In a previous work, we demonstrated that HBpin is capable of reducing Ni(acac)₂ in the presence of XantPhos to give Ni(0) species **II** and molecular hydrogen (Scheme 5, bottom).^[11a]

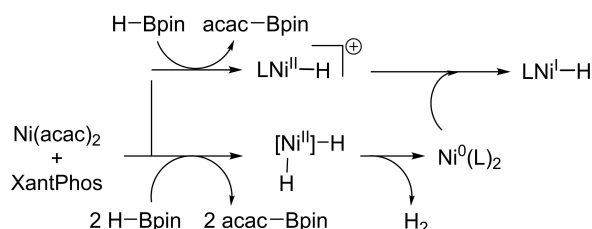
On the other hand, the yields of the cycloisomerization reactions decrease when using a 1:1 ratio of HBpin to Ni(II), which suggests that Ni–H species are not reactive intermediates, and that a full reduction of the precatalyst to Ni(0) is necessary (Scheme 5, bottom). We also considered the possibility of the



Scheme 3. Reaction involving an internal alkyne.



Scheme 4. ^aA minor non-identified isomer is present. Yield estimated by NMR. ^bContaminated with a non-identified compound.



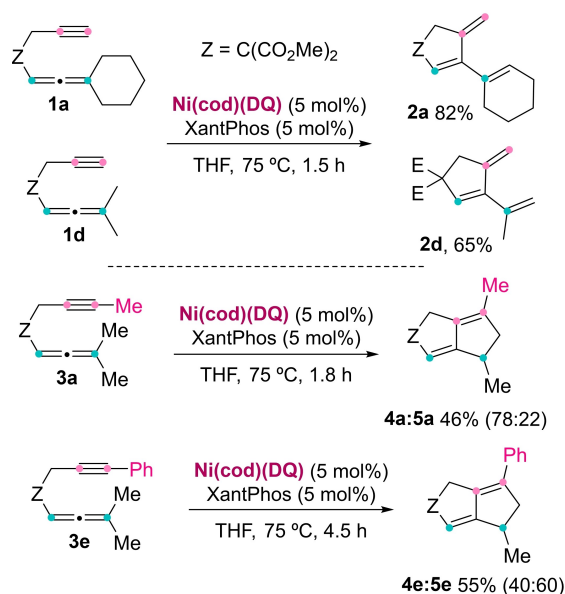
Scheme 5. Hypothetical intermediate Ni complexes.

formation of Ni(I) species by Ni(0) and Ni(II) comproportionation (Scheme 5, top), but intermediacy of this kind of species can be disregarded for several reasons: two different mechanisms would have to occur for the formation of products **4** and **5**, and 1,2-insertions processes could hardly take place (see Supporting Information for details). Moreover, the cycloisomerization of **1a**, **1d**, **3a**, and **3e** with Ni(0) complex Ni(cod)(DQ) (DQ = duroquinone), and XantPhos took place in the absence of HBpin (Scheme 6). In all cases, the desired products were obtained. Reaction of substrates with internal alkynes gave lower **4:5** ratios. However, the lower yields obtained make it

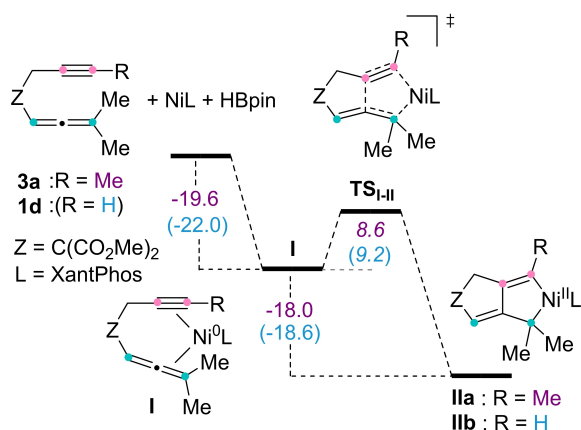
difficult to compare the selectivities with the Ni(II)/HBpin catalyzed reactions. Reaction of **3e** needed a longer time for completion, which may lead to partial decomposition of the bicycle, as we observed during the optimization of the reaction conditions mentioned above. The difference in selectivity may be also related to the presence of DQ ligand. These experiments suggest that Ni(0) is the actual catalyst, and that alternative Ni sources can be also used.

In summary, coordinatively unsaturated Ni(0)(XantPhos) complex is the most likely catalytically active species, as we already proposed for the borylative cyclization of enynes and the borylative bicyclization of allenynes.^[12a,d] Coordination of the allenene would trigger an oxidative cyclometalation as the first reaction step.

We have performed DFT calculations to explore the feasibility of this process and to try to depict a full reaction pathway.^[16] Full structures of **3a**, **1d**, and XantPhos have been used as models (Scheme 7). Activation of the substrates proceeds by exoergic coordination of **3a** and **1d** to Ni(XantPhos) give 16-electron complexes **I** (−19.6 and −22 kcal·mol^{−1}, respectively), followed by a low barrier (8.6 and

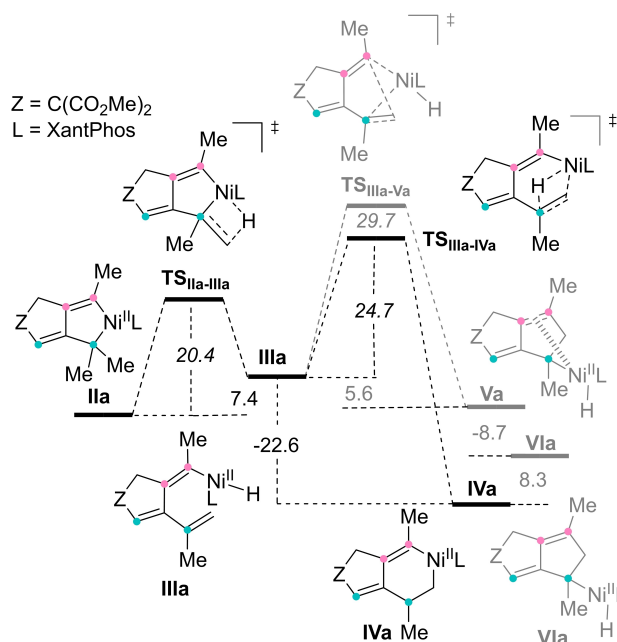
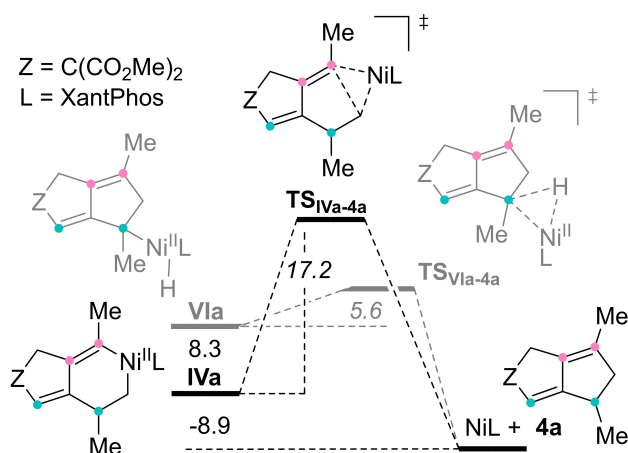


Scheme 6. Ni(0)-catalyzed cycloisomerizations.

Scheme 7. Calculated reaction, activation and relative ΔG ($\text{kcal}\cdot\text{mol}^{-1}$) for coordination and oxidative cyclometalation reactions from **1d** (in brackets) and **3a** (ΔG_a in italics).

$9.2 \text{ kcal}\cdot\text{mol}^{-1}$) and thermodynamically favorable oxidative cyclometalations (-18.0 and $-18.6 \text{ kcal}\cdot\text{mol}^{-1}$), generate diorgano-nickelacycles **II**.

Complexes **IIa** and **IIb** evolve through similar pathways. For clarity, results for the substrates derived from internal alkynes are shown in Schemes 8 and 9 (see Supp. Information for details concerning **IIb** and subsequent calculated intermediates and energies). Nickelacycle **IIa** experiences β -hydrogen elimination to give Ni–H complex **IIIa**. This process is endoergic ($7.4 \text{ kcal}\cdot\text{mol}^{-1}$) but shows an accessible reaction barrier at the reaction temperature ($20.4 \text{ kcal}\cdot\text{mol}^{-1}$) and is followed by an exergonic irreversible insertion reaction.

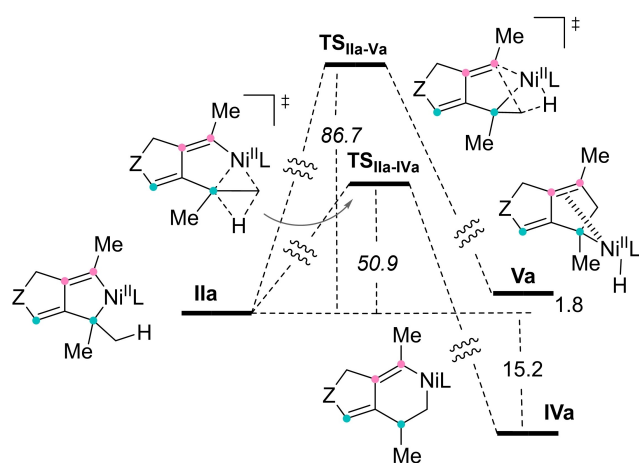
Scheme 8. Calculated reaction, activation and relative ΔG ($\text{kcal}\cdot\text{mol}^{-1}$) for β -hydrogen elimination from **IIa** and subsequent possible 1,2-insertion reactions (ΔG_a in italics).Scheme 9. Calculated reaction, activation and relative ΔG ($\text{kcal}\cdot\text{mol}^{-1}$) for C–C reductive elimination reactions (ΔG_a in italics).

We have calculated the two possible 1,2-insertion reactions that may occur from complex **IIIa**, due to the *cis* arrangement between the intervening ligands: carbometallation of the coordinated alkene by the Ni-alkenyl bond and hydrometallation of the alkyne involving the Ni–H bond. The latter process shows a lower activation free energy compared to the carbometallation (24.7 vs $29.7 \text{ kcal}\cdot\text{mol}^{-1}$), and therefore, six-membered metallacycle **IVa** should better be formed, instead of the five-membered complex **Va** (which shows an initially coordinated alkene and dissociates

to more stable intermediate **VIa**). The preferred hydrometallation is highly exoergic and, in consequence, irreversible (calculated activation free energy for the back reaction is $47.3 \text{ kcal} \cdot \text{mol}^{-1}$). We propose complex **IVa** as the actual reaction intermediate. Evolution through C–C reductive elimination from either diorgano-nickel derivative would take place then spontaneously with low activation barriers and have no influence neither in the reaction outcome or the kinetics (Scheme 9).

The calculated activation energy for the hydrometallation reaction is relatively high, but it may be compatible with the reaction conditions within the error of the computational approach. Nevertheless, we have explored alternative mechanisms for the evolution of complex **IIa** avoiding the insertion reactions of the alkene into the Ni–H or Ni–C bonds. We have been able to locate two transition states that would afford either **IVa** or **Va** directly from **IIa**. Dyotropic rearrangement of Ni and H through $\text{TS}_{\text{IIa-IVa}}$ shows a very high activation energy ($50.9 \text{ kcal} \cdot \text{mol}^{-1}$, Scheme 10). Alternative methyl C–H activation with concomitant formation of a C–C bond with the alkenyl ligand is also impossible (activation free energy $86.7 \text{ kcal} \cdot \text{mol}^{-1}$). Therefore β -elimination to complexes **III** is the most feasible mechanism.

Interestingly, the geometry imposed by the ancillary ligand in **IIIa** forces the hydride to lie trans to the alkenyl-Ni bond, which precludes a fast C–H reductive elimination. Otherwise, this process would immediately occur leading to the formation of trienes **2** and **5**, and bicyclic products could not be formed. However, reaction involving allenes containing a terminal alkyne (**1a–g**) do not afford bicyclic derivatives, indicating that a faster reaction compared to hydrometallation of the alkene in complex **IIIb** must be taking place, leading to products **2**. We have been able to calculate a transition state (TS) for the isomerization

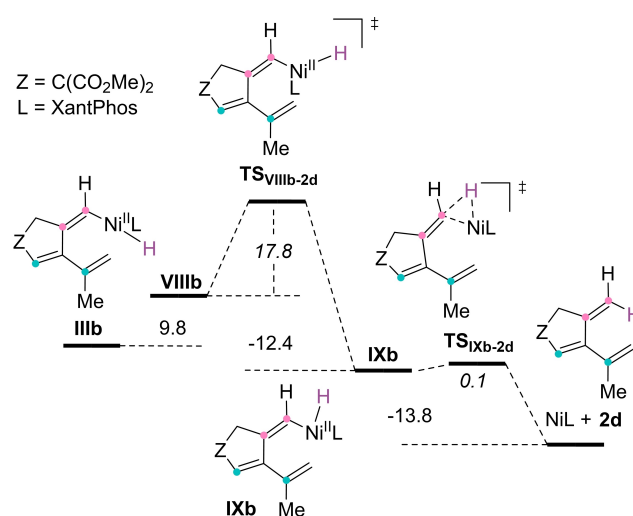


Scheme 10. Energy profile for alternative (impossible) mechanisms (ΔG_a in italics).

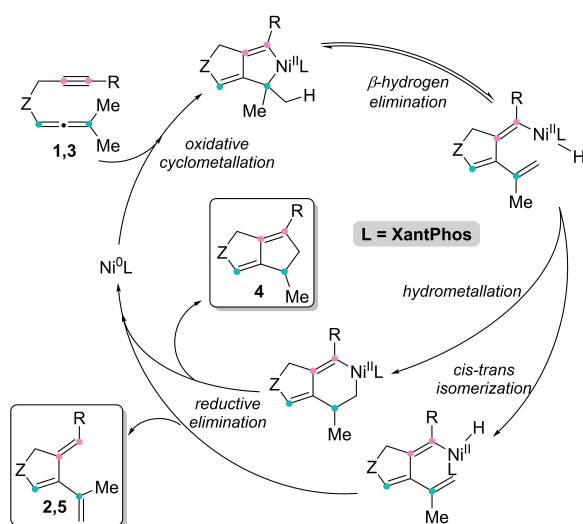
of the trans alkenyl-Ni–H complex **IIIb** which leads to a cis derivative by bending the C–Ni–H bond from 174° to 76° (Scheme 11).

Intrinsic reaction coordinate calculations show that isomerization starts with the elongation of one of the Ni–P bonds from **IIIb** (Ni–P distance, 2.56 \AA) to give a less stable complex **VIIIb** ($+9.8 \text{ kcal} \cdot \text{mol}^{-1}$, Ni–P distance, 3.10 \AA) which evolves to give the cis isomer through $\text{TS}_{\text{VIIIb-IXb}}$, with a $17.8 \text{ kcal} \cdot \text{mol}^{-1}$ barrier.

Analogous transition state for the cis-trans isomerization from **IIIa** could not be found, since the interaction of the methyl group in the initial alkyne fragment with the XantPhos ligand precludes convergence of the calculation to a saddle point in the potential energy surface (see Supporting Information). Although $\text{TS}_{\text{VIIIb-IXb}}$ shows a slightly higher energy compared to the hydrometallation TS ($2.2 \text{ kcal} \cdot \text{mol}^{-1}$), we propose, within the error of the calculations, that this isomerization accounts for the formation of cis alkenyl-Ni–H complexes, which provide the formation of monocyclic trienes **2** and **5** by a fast C–H reductive elimination. We have therefore a plausible explanation for the different outcome of the reaction (Scheme 12) depending on the structure of the substrate (terminal or internal alkyne) that is related to the special structure of the XantPhos ligand, and the restrictions imposed in the coordination sphere. It is especially relevant the direct formation of kinetically stable C–Ni–H trans complexes derived from substrates containing internal alkynes. These hydride complexes evolve through carbometallation of the alkene to give the second ring, but isomerization to the cis derivative (which gives a fast C–H reductive elimination) competes at some extent, explaining the formation of the minor monocyclic products and, therefore, the absence of complete selectivity.



Scheme 11. Calculated reaction profile for the isomerization and C–H reductive elimination ($\Delta G \text{ kcal} \cdot \text{mol}^{-1}$, ΔG_a in italics).



Scheme 12. Summary of the proposed reaction pathways.

Conclusion

In summary, we have developed wide-scope Ni-catalyzed cycloisomerizations of 1,5-allenyne that afford either mono- or bicyclic derivatives depending on the structure of the starting compounds. The formation of fused 5–5 derivatives from internal alkynes is especially relevant since two C–C bonds are formed in a single synthetic operation in which a C–H bond is previously activated. Reactions are fully atom-economical. Our experimental and computational studies have allowed us to propose a reaction pathway with interesting features that explain the observed selectivity.

Experimental Section

A vial was charged with the corresponding 1,5-allenyne (1.0 equiv), $\text{Ni}(\text{acac})_2$ (5 mol%) and XantPhos (5 mol%) and backfilled with Argon. Then, anhydrous and Ar-degassed THF (0.1 M) was added under an inert atmosphere. The mixture was stirred for 5 min, and HBpin (15 mol%) was added, observing a colour change to yellow-orange. The mixture was left stirring for 1.5 with allenyne **1** or 4 h with allenyne **3** at 75 °C. The crude reaction was filtered through silica gel washing with Cy/EtOAc (7:3). The solvent was removed under vacuum and the residue was purified by column chromatography.

Author Contributions

J. C. N.-C. and I. M.-M. contributed equally to this work.

Acknowledgements

We thank the support by MICIU (CTQ2016-79826-R and PID2019-109088GB-I00) and for FPI fellowships to J. C. N.-C., I. M. M. and G. C.-S. We also thank the Centro de Computación Científica-UAM for technical assistance.

References


- [1] a) C. Aubert, L. Fensterbank, P. Garcia, M. Malacria, A. Simonneau, *Chem. Rev.* **2011**, *111*, 1954–1993; b) T. Wang, J.-X. Guan, Y.-X. Tan, P. Tian, *Org. Lett.* **2023**, *25*, 5935; c) Y. Zhang, W. Xu, T. Gao, M. Guo, C.-H. Yang, H. Xie, X. Kong, Z. Yang, J. Chang, *Org. Lett.* **2022**, *24*, 7021; d) H. Komatsu, T. Ikeuchi, H. Tsuno, N. Arichi, K. Yasui, S. Oishi, S. Inuki, A. Fukazawa, H. Ohno, *Angew. Chem. Int. Ed.* **2021**, *60*, 27019; e) X. Deng, L.-Y. Shi, J. Lan, Y.-Q. Guan, X. Zhang, H. Lv, L. W. Chung, X. Zhang, *Nat. Commun.* **2019**, *10*, 949; f) S. H. Sim, S. I. Lee, J. Seo, Y. K. Chung, *J. Org. Chem.* **2007**, *72*, 9818; g) N. Cadran, K. Cariou, G. Hervé, C. Aubert, L. Fensterbank, M. Malacria, J. Marco-Contelles, *J. Am. Chem. Soc.* **2004**, *126*, 3408.
- [2] a) N. Saito, Y. Kohyama, Y. Tanaka, Y. Sato, *Chem. Commun.* **2012**, *48*, 3754–3756; b) L. M. Joyce, M. A. Drew, A. J. Tague, T. Thaima, A. Gouranourimi, A. Arifard, S. G. Pyne, C. J. T. Hyland, *Chem. Eur. J.* **2022**, *28*, e202104022; c) C. Mukai, F. Inagaki, T. Yoshida, K. Yoshitani, Y. Hara, S. Kitagaki, *J. Org. Chem.* **2005**, *70*, 7159.
- [3] Selected references: a) T. Gillmann, T. Hülsen, W. Massa, S. Wocadlo, *Synlett* **1995**, 1257–1258; b) M. E. Cinar, C. Vavilala, J. Fan, M. Schmitt, *Org. Biomol. Chem.* **2011**, *9*, 3776–3779; c) M. Schmitt, C. Vavilala, *J. Org. Chem.* **2005**, *70*, 4865–4868; d) T. Bekele, C. F. Christian, M. A. Lipton, D. A. Singleton, *J. Am. Chem. Soc.* **2005**, *127*, 9216–9223; e) M. Schmitt, A. A. Mahajan, G. Bucher, J. W. Bats, *J. Org. Chem.* **2007**, *72*, 2166–2173; f) C. Vavilala, J. W. Bats, M. Schmitt, *Synthesis* **2010**, *13*, 2213–2222; g) D. Samanta, M. E. Cinar, K. Das, M. Schmitt, *J. Org. Chem.* **2013**, *78*, 1451–1462; h) D. Samanta, A. Rana, M. Schmitt, *J. Org. Chem.* **2015**, *80*, 2174–2181.
- [4] a) G.-Y. Lin, G.-Y. Yang, R.-S. Liu, *J. Org. Chem.* **2007**, *72*, 6753–6757; b) P. H.-Y. Cheong, P. Morganelli, M. R. Luzung, K. N. Houk, F. D. Toste, *J. Am. Chem. Soc.* **2008**, *130*, 4517–4526; c) M. Wegener, S. F. Kirsch, *Org. Lett.* **2015**, *17*, 1465–1468; d) T. Ikeuchi, S. Inuki, S. Oishi, H. Ohno, *Angew. Chem. Int. Ed.* **2019**, *58*, 7792–7796; e) H. Komatsu, T. Ikeuchi, H. Tsuno, N. Arichi, K. Yasui, S. Oishi, S. Inuki, A. Fukazawa, H. Ohno, *Angew. Chem. Int. Ed.* **2021**, *60*, 27019–27025.
- [5] a) R. Zriba, V. Gandon, C. Aubert, L. Fensterbank, M. Malacria, *Chem. Eur. J.* **2008**, *14*, 1482–1491.
- [6] C. H. Oh, A. K. Gupta, D. I. Park, N. Kim, *Chem. Commun.* **2005**, 5670–5672.
- [7] a) K. M. Brummond, D. Chen, T. O. Painter, S. Mao, D. D. Seifried, *Synlett* **2008**, *5*, 759–764; b) K. M.

- Brummond, B. Yan, *Synlett* **2008**, 15, 2303–2308; c) F. Inagaki, K. Sugikubo, Y. Oura, C. Mukai, *Chem. Eur. J.* **2011**, 17, 9062–9065; d) Y. Oonishi, T. Yokoe, A. Hosotani, Y. Sato, *Angew. Chem. Int. Ed.* **2014**, 53, 1135–1139.
- [8] a) L. Peng, X. Zhang, J. Ma, J. Wang, *Org. Chem. Front.* **2014**, 1, 235–239; b) L. Peng, X. Zhang, M. Ma, J. Wang, *Angew. Chem. Int. Ed.* **2007**, 46, 1905–1908; c) L. Peng, X. Zhang, M. Ma, J. Wang, *J. Organomet. Chem.* **2011**, 696, 118–122.
- [9] Z. Zheng, L. Deiana, D. Posevins, A. A. Rafi, K. Zhang, M. J. Johansson, C. Tai, A. Córdova, J.-E. Bäckvall, *ACS Catal.* **2022**, 12, 1791–1796.
- [10] a) D. J. Gorin, B. D. Sherry, F. D. Toste, *Chem. Rev.* **2008**, 108, 3351–3378; b) A. C. Reiersolmøen, D. Csókás, A. Fiksdahl, M. Elderyi, *J. Am. Chem. Soc.* **2019**, 141, 18221–18229; c) C. Nieto-Oberhuber, S. López, A. M. Echavarren, *J. Am. Chem. Soc.* **2005**, 127, 6178–6179.
- [11] N. Cabrera-Lobera, P. Rodríguez-Salamanca, J. C. Nieto-Carmona, E. Buñuel, D. J. Cárdenas, *Chem. Eur. J.* **2018**, 24, 784–788.
- [12] a) N. Cabrera-Lobera, M. T. Quirós, E. Buñuel, D. J. Cárdenas, *Catal. Sci. Technol.* **2019**, 9, 1021–1029; b) N. Cabrera-Lobera, M. T. Quirós, W. W. Brennessel, M. L. Neidig, E. Buñuel, D. J. Cárdenas, *Org. Lett.* **2019**, 21, 6552–6556; c) N. Cabrera-Lobera, M. T. Quirós, E. Buñuel, D. J. Cárdenas, *Chem. Eur. J.* **2019**, 25, 14512–14516; d) I. Manjón-Mata, M. T. Quirós, E. Velasco-Juárez, E. Buñuel, D. J. Cárdenas, *Adv. Synth. Catal.* **2022**, 364, 1716–1723.
- [13] H. Li, J. Zhang, X. She, *Chem. Eur. J.* **2020**, 27, 4839–4858.
- [14] G. J. Kramp, M. Kim, H. -J. Gais, C. Vermeeren, *J. Am. Chem. Soc.* **2005**, 127, 17910–17920.
- [15] Y. Chen, J. Shi, L. Li, F. Liu, X. Zhang, Y. Yang, *Tetrahedron Lett.* **2021**, 62, 152627.
- [16] Calculations were performed at M06-2X/6-31G(d) (C,H,O,P), LANL2DZ (Ni) level. Optimizations were performed in THF (PCM model). See Supporting Information for details.
- [17] According to the Eyring-Polanyi equation, we would expect an activation free energy of 22.4 kcal mol⁻¹ for a reaction showing a half-reaction time of 1 h.

RESEARCH ARTICLE

Nickel-Catalyzed Cycloisomerization of 1,5-Allenynes

Adv. Synth. Catal. **2023**, 365, 1–9

 J. C. Nieto-Carmona, I. Manjón-Mata, M. T. Quirós*, G. Caballero-Santiago, F. Pérez-Maseda, D. J. Cárdenas*

